DESIGN FOR OPERATION

Kirsten Odendaal, Luigi Francesco Minerva – MARIN, The Netherlands
Giedo Loeff – Feadship, The Netherlands

SUMMARY

As the industry has a need for more efficient and fuel-flexible solutions, there is a growing desire to shift away from specification (contractual) design and more towards data-driven operational design. For the yachting market, this translates into extending leisure at sea while ensuring the demands for lower fuel consumption, increased operational efficiency, and higher degrees of comfort. To ensure these expectations can be achieved, the functional usage of the yacht has to be investigated during the early design phases, and performance has to be tuned to fit-the-use. However, current hull form optimisation practices are usually presented only in terms of hydrodynamic resistance reduction to fulfill (sometimes arbitrary) maximum speed and range requirements in unrealistic seagoing conditions governed by contractual constraints. Unfortunately, based on extensive data monitoring studies, yachts typically operate only a fraction of their operational life at these top speeds and in those conditions. Therefore, these vessels commonly function in regions where the optimisation process is not focused, and consequently, the hydrodynamic efficiency is much lower than expected (influencing vital operational metrics such as vessel range and cost). Therefore, the paper's objective is to show the impact on the hull form design once the operational profile and conditions are taken into account. In that respect, a re-optimisation process of two existing Feadship yachts is carried out based on implementing data-driven operational profiles and seagoing conditions. Operating cost, environmental impact and performance will be assessed considering the lifecycle.

1. INTRODUCTION

Within the superyacht industry, there is an increasing awareness of environmental and societal impacts caused by the various life phases of a superyacht. Understanding, identifying and mitigating all these impacts can be rather complex; however, some significant reductions are very straightforward. Subject to this study, and perhaps the most obvious, is energy efficiency optimisation by specification of the actual use/load profiles. This study will show that substantial fuel consumption and associated emission and cost reductions can be achieved while using operational feedback from the existing fleet. It merely a redefinition of the design specification and modified design process with some potential aesthetic and design trade-offs.

The principle of operation-based design is relevant for all systems onboard. The energy consumption of a superyacht can be split into the propulsion and auxiliary "hotel" load, representing on average, equal annual energy consumption shares. This study is limited to optimisation of the propulsion load based on the relevant sailing profile and sea conditions. Nevertheless, optimisation of significant hotel loads such as the heating, ventilation and air conditioning (HVAC) system, which can be based on the actual climate conditions, can be considered equally important.

The study under consideration is based on two existing Feadships currently in operation. Based on the actual sailing profile and sea climate observed, the hull shapes have been re-optimised within reasonable design boundary conditions. The optimisation is conducted using a surrogate-based multi-objective method utilizing RANS-CFD code for calm water resistance estimation and a panel-theory code to determine the added resistance in waves. The two subject vessels have been re-optimised using a different approach. One yacht (subject A) has been optimised using a course approach, representative of an early design phase, typically before the build contract phase. In contrast, the other yacht (subject B) has been optimised in greater detail, commonly considered a basic design refinement phase.

The use profile, optimisation method and results are presented in this paper. The gains have been presented in terms of power-speed impact reductions, and cost comparisons have been drawn when considering other impact-reducing measures.
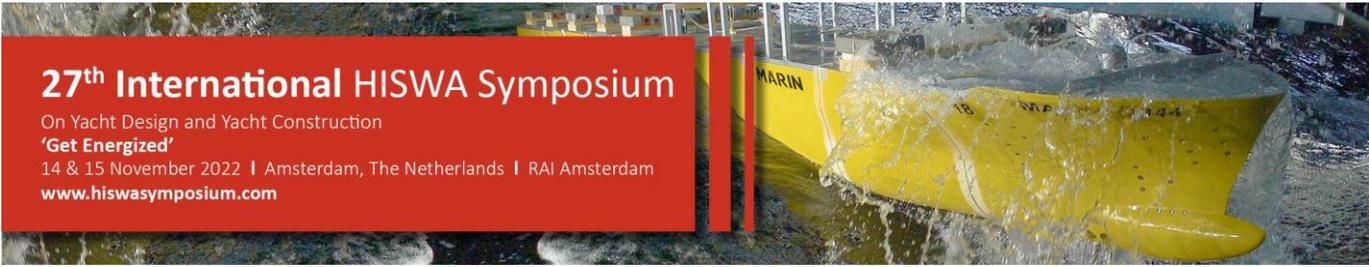
2. USE PROFILE

Use profile information is derived from Feadship's 7SEAS framework, interfacing both ample automated identification system (AIS) and metocean weather model data (ECMWF). For the sake of this study, the sailing profiles of both subject vessels have been considered an average of the two yachts, allowing for a more consistent comparison. However, superyachts do not have a fixed operational profile. The actual average time spent sailing can significantly vary between 1% to 25% of the year (see Figure 1 for a reduced set of Feadship yachts). Amounting from some 3.000 to 25.000 nautical miles sailed a year, ranging from local cruising in the Mediterranean to global explorations around all continents. Therefore, the question is whether to optimise for an average user profile or a user-specific intended profile. Both approaches could work and are, in principle, decoupled from the methodology presented here. One may argue that a series-produced yacht or a client without specific intended use could best design for a mean profile. However, other clients of custom-designed yachts may already have a particular use in mind or have been using a yacht for years. Those clients may reduce their impacts and related costs from user-specific use profiles.
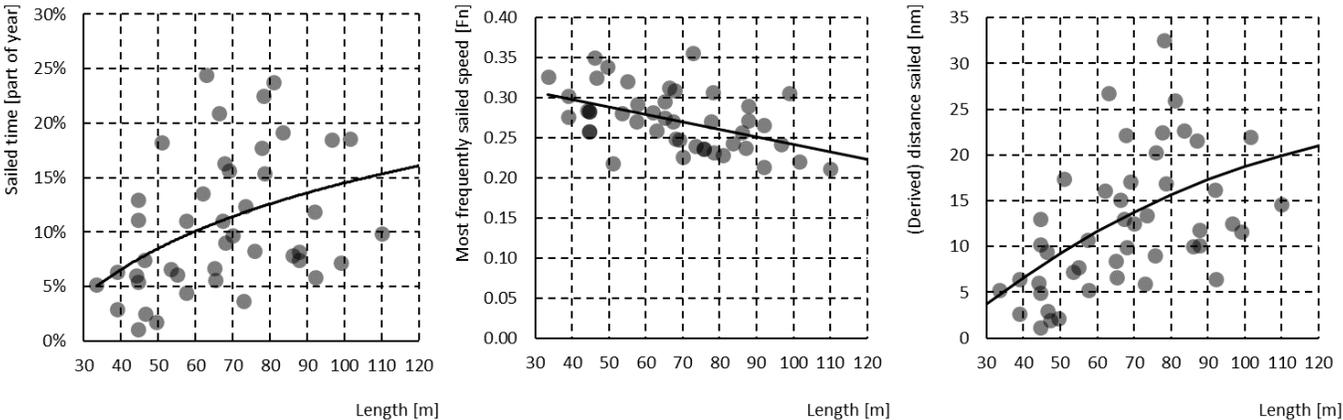
Figure 1: Yacht sailing profile statistics

The most dominant profile characteristic within the context of this study is the most frequently sailed speed. As can be derived, the relative speed (Froude number, Fn) reduces with increasing size. The sailed time also increases, causing the related impact to grow relatively with yacht size.

2.1 Speed profile

Bearing in mind the considerations posed before, for the sake of this study, the mean sailing profile of the two subject vessels was determined. For practical numerical reasons, three speeds are determined to consider in the surrogate-based multi-objective. The chosen speeds are based on the individual operational analysis for both vessels:

Yacht A: $V_{s,A}$ = 12, 15, 18 knots ($\text{Froude}_{\text{Lpp,A}}$ = 0.20, 0.25, 0.30)
Yacht B: $V_{s,B}$ = 13, 15, 18 knots ($\text{Froude}_{\text{Lpp,B}}$ = 0.25, 0.28, 0.34)

Figure 2 provides the analysed speed profiles, indicating both vessels objective speeds and the proportions spent at each speed as 85%, 14% and 1%, respectively. The weighting for yacht B was deliberately modified to resemble yacht A since the sailing statistics of yacht B were insufficient. These three speeds relate to respectively the speeds sailed during ocean crossing/migration, cruising and top speed.

27th International HISWA Symposium

On Yacht Design and Yacht Construction
'Get Energized'
14 & 15 November 2022 | Amsterdam, The Netherlands | RAI Amsterdam
www.hiswasymposium.com

Figure 2: Speed profile, yacht A (left), yacht B (right).

2.2 Environmental profile

The mean sea climate is determined by matching AIS and metocean model data for the moments Feadships are sailing. Since long-term statistics are required, it is decided to use a more extensive fleet (60 Feadship spread over a period of some 10 years) to determine the wave statistics. In **Error! Reference source not found.**, the scatter diagram is provided showing the probability of occurrences of significant wave height and peak period combinations.

Wave height [m]												
3.25										0.0%		
2.75								0.0%	0.0%	0.0%	0.1%	
2.25			0.0%	0.2%	5.4%	1.1%	0.9%	0.4%	0.6%	0.5%	0.2%	
1.75		0.3%	2.1%	4.6%	9.0%	5.5%	2.7%	1.0%	0.7%	1.6%	0.2%	
1.25	0.0%	0.9%	10.4%	7.0%	9.7%	12.0%	8.7%	1.1%	2.3%	0.4%	0.0%	
0.75	0.4%	1.3%	0.9%	1.1%	3.3%	1.0%	1.6%	0.0%	0.0%	0.0%	0.0%	
0.25	0.2%	0.0%	0.0%	0.1%	0.0%	0.0%	0.0%	0.0%	0.0%	0.0%	0.0%	
	3.5	4.5	5.5	6.5	7.5	8.5	9.5	10.5	11.5	12.5	13.5	14.5

Peak period [s]

Probability of occurrence of wave system while sailing

Figure 3: Scatter diagram for Feadship fleet while sailing

For the sake of reduction of numerical capacity requirements, the decomposition into wind sea and swell as well as relative wave headings are neglected. Thus, the wave impacts are computed only for head seas in a most probable encountered sea-going condition with a peak period of 8.5s and wave height of 1.25m. Additional improvements, such as alternative conditions and headings, may be included in the future. The operational data is available.

3. METHODOLOGY AND ESTABLISHED RESEARCH

Figure 4 presents our optimisation procedure in schematic form. Each block is labelled with a number for reference purposes in the remainder of this paper. In the following subsections the main blocks of this methodology are described in more details.
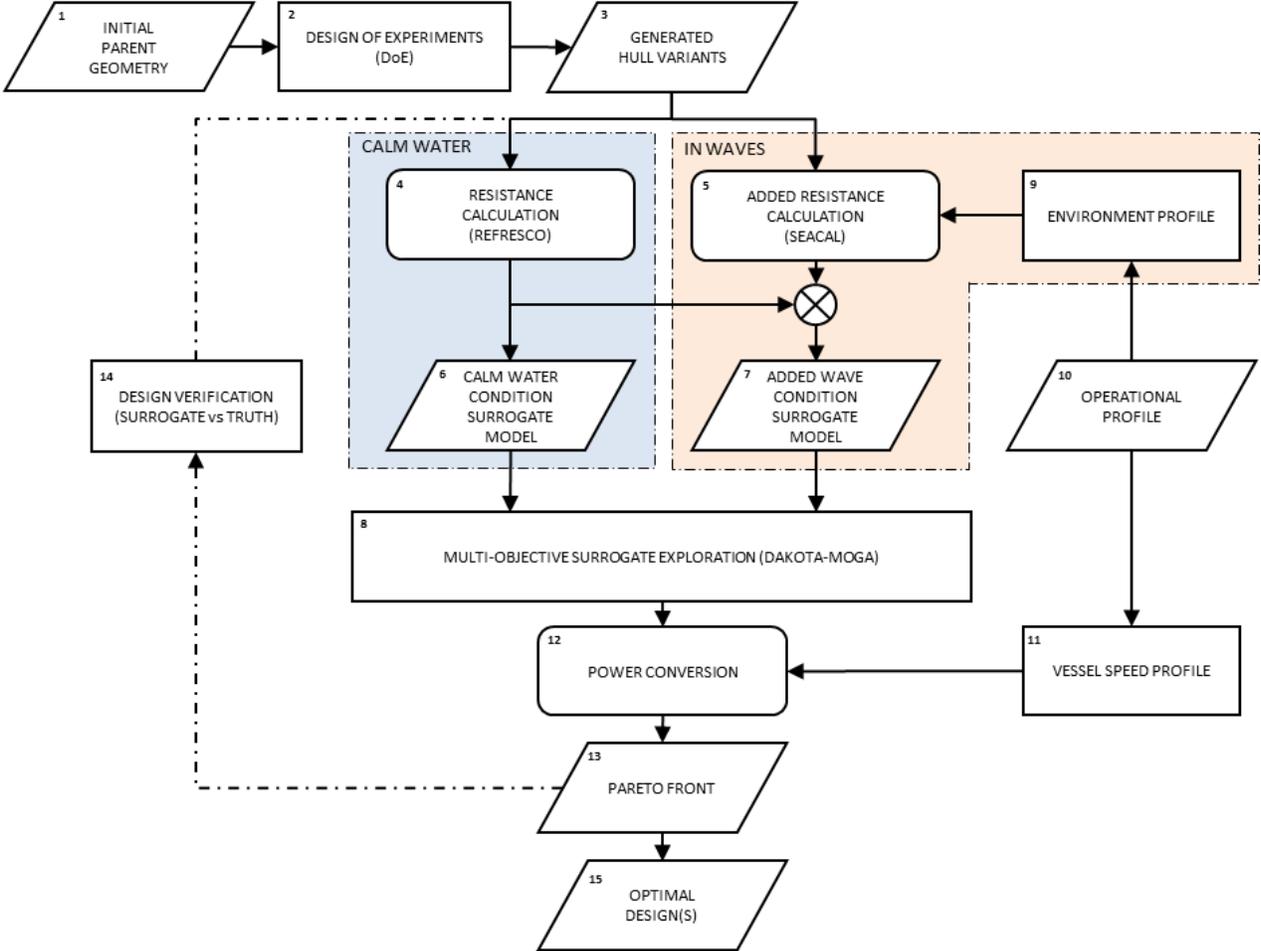
Figure 4: Flowchart of surrogate-based multi-objective optimisation for calm water and in wave condition performance.

As shown in the above flow diagram, two possible path ways can be integrated. The first one is the approach of conventional hull form optimisation which considers only calm water conditions. The second approach aims to consider true operational or realistic conditions and the impact environmental conditions have on the end result of the hull form optimisation process. Where the first is considered a traditional design approach, the latter is considered as on-going research given the unique challenge to combine multiple aspects and disciplines to explore the impacts of operational design on hull form shape and energy use. In this specific study, only impacts of wave added resistance will be investigated since this is predominantly the largest contributor when compared to wind and hull fouling components [4]. However, to account for such additional operational components, they can be simply included within the added resistance calculation (block 5).

27th International HISWA Symposium
On Yacht Design and Yacht Construction
'Get Energized'
14 & 15 November 2022 | Amsterdam, The Netherlands | RAI Amsterdam
www.hiswasymposium.com

MARIN

3.1 Parametric geometry modelling

The first blocks (1, 2 and 3) focus on apply hull-blending techniques which are used to parameterize the parent hull geometry. The associated details such as hull geometry features and design constraints within the relevant ship characteristics in combination with general arrangement and propulsion system information. Once relevant ship aspects are defined within the indicated constraints, a small number of hull designs, named "extreme variant", are developed. These variants are featured with extreme versions of the selected ship aspects and they define the allowable modifications the parent hull can under go.

As detailed by [10], if one of these basis designs is appointed as the 'original' parent design D_O, then the other extreme variants $D_1, D_2, \ldots, D_M$ are the 'alternative' designs. We assume that the shape of each D_M is defined by N_c control points $(x_{M,i})$ of a B-spline surface. In step 2, a Design of Experiments (DoE) is created from this parameterized hull shape: the correspondent parameterized control points $x_i(d)$ are obtained by linear interpolation on those of the extreme variants:

$$x_i(d) = x_i([d_1, d_2, \ldots, d_m]) = x_{0,i} + \sum_{m=1}^{M} d_m(x_{m,i} - x_{0,i}) \quad \text{for } i = 1,2, \ldots, N_c \qquad (1)$$

Each linear interpolation coefficient d_m represents the contribution of the corresponding extreme variant design D_M in the hull 'blend'. Further details related to the blending process can be found in [7], [8], and [10]. Once the initial hull is parameterized with the extreme variants, a sampling routine is applied to generate a sufficient number of geometries which can adequately cover the design space. In this study, the sampling procedure used is the Latin Hypercube Sampling (LHS). LHS is a statistical method for generating a near-random sample of parameter values from a multidimensional distribution. The number of samples (S) required to adequately populate the design space can be predicted using the formulation below:

$$S = \frac{(n + d)!}{n! \, d!} \qquad (2)$$

Where the n is the number of design variables and d is the dimension or fidelity factor. The lower the fidelity solver, the lower the dimension. Solvers with high computational demand (such as RANS codes) are typically set at 2. In addition, the extreme variants are also included in the sample set. This allows for the design space to be adequately represented at the extreme boundary positions. In this study the hull blending is implemented in Rhino's algorithmic modelling tool Grasshopper [9] and forms the geometric basis for the combined calm-water and in waves optimisation.

3.2 Numerical methods and mathematical formulations

This section describes the numerical tools used for the optimisation studies. The total resistance (R_T) of a vessel can be decomposed into multiple components. However, two components typically dominate the total resistance: the calm water resistance (R_{CW}) and the added resistance (R_A). Typically the latter is a result of external factors such as waves or wind conditions which may adversely influence the performance of a vessel. Thus, the total resistance of ships in realistic operations may be expressed as following,

$$R_T = R_{CW} + R_A \qquad (3)$$

To account for these components, the methodology is split in a workflow that generates an input for MARIN's viscous flow RANS-CFD code ReFRESCO and a workflow that generates the input for MARIN's panel theory code SEACAL, respectively used to compute the resistance in calm water and in waves. The ReFRESCO input contains a surface triangularization (STL) of the CFD domain and the variant hydrostatics, whereas the geometry panel file are the required input for SEACAL. Further technical details of both ReFRESCO and SEACAL can be found in [5] and [6], respectively. The outcome of the calm water (steps 4 and 6) and in waves (steps 5 and 7) modelling workflows is then coupled to the open-source tool DAKOTA [1]. In this tool there is a large variety of optimisation algorithms. In this study, a genetic algorithm is used to identify optimum cases from the surrogate models derived for the total resistance (chosen as objective function) of the calm water and in waves conditions. Further details are given in the subsection
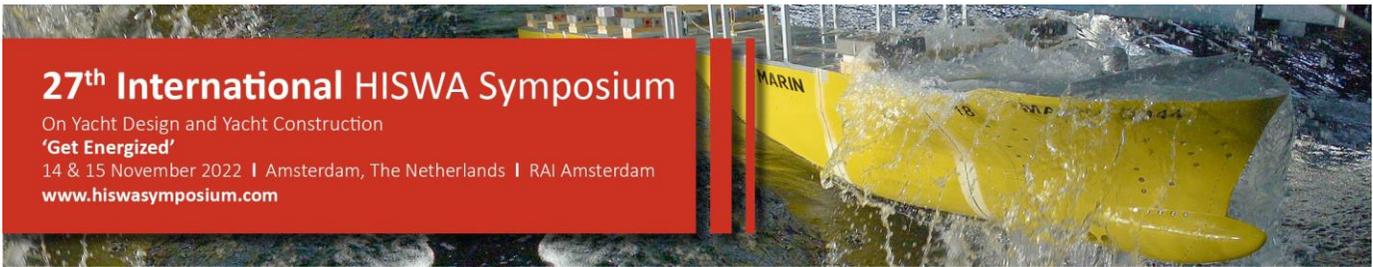
3.4. At this point, the total resistance objective function can be extracted or further converted into power and/or other operational contributions (such as achievable nautical mile range and/or fuel consumption).

3.3 SEACAL Modelling uncertainties

When investigating hull shapes including the interaction with waves, there are two aspects to take into account: one related to the additional physical phenomena, such as splashing of a re-entrant bow (especially with bulb) or the bow slamming; another one related to the numerical model behind SEACAL itself. Therefore, it should be also noted that while SEACAL is used to assess the resistance in waves, other techniques and tools of varying fidelities can be used as well. Thus, much like the calm-water resistance, the proposed methodology is a flexible framework which can incorporated other fidelity tools regardless of the state of the design.

Regarding the limitations of the numerical model, SEACAL is a Panel theory code. As such, the variation and quality of panel distributions have the potential to influence the results which can be highly sensitive to panel stretching. While, SEACAL is a generally robust tool, its integration with parameter hull-blending approaches has not been investigated. Thus, results using the proposed methodology have yet to be explicitly validated. Beyond the aforementioned numerical source of uncertainty, there are also additional physical aspects influencing the identification of the optimal hull form when interaction with waves is included: local flow features (such as bulb re-entry) can have an impact on the selection of the optimal hull shape. Additionally, other bow characteristics, such flairs or bulbs, can influence the slamming behaviour and eventually lead to different decisions regarding the shape of the hull. However, such phenomenon is not fundamentally considered within SEACAL and therefore it does not play a role in the optimisation implemented in the described methodology.

3.4 Multi-objective surrogate optimisation

There are many optimisation procedures used to identify an ensemble of optimal solutions (so called Pareto front), in a wide variety applications. However, as detailed by [8], direct multi-objective optimisation is often much too expensive for practical design applications. Therefore, it is necessary to select a suitable strategy that can reduce the computational cost efficiently. In this applied research, surrogate models, which are much cheaper to evaluate, are thus used instead. These meta models are constructed from a number of direct evaluations on pre-defined designs generated (from sampling plans such as LHS) which represent the geometry variations in the design space; the Design of experiments (DOE) [10]. In addition to be being a cheaper solution, the models themselves can be easily enriched with new information to quickly improve accuracy or reduce modelling noise. Once the new direct evaluations are identified, a surrogate model can be re-trained on the enriched sampling dataset. Therefore, multiple iteration loops can be considered in the design optimisation phase, where each optimal surrogate solution can be re-evaluated and included in the next sampling set to further enhance the corresponding accuracy. In this study, surrogates are constructed using Kriging for the calm-water resistance and total added resistance (thus including resistance in waves), respectively. The construction of the Kriging surrogate models is internally available from DAKOTA.

Multi-objective optimisation based on the surrogate response surfaces is used to find Pareto-optimal solutions. The Pareto front shows the trade-off between calm-water resistance and total added resistance objectives at the various speeds of interest. Here, DAKOTA's Multi-Objective Genetic Algorithm (MOGA) algorithm is used to obtain the Pareto front. These algorithms the ability to avoid being trapped in local optimal solution like traditional methods, which search from a single point. However, they typically require large numbers of evaluations to ensure an optimum is reached [3]. Therefore, the combination of MOGA and surrogate models (step 8) to reduce the computational expense provides a highly efficient and feasible design procedure for all stages of design procedures.

3.5 Operational powering assessment

Typically, once an optimisation is completed, the point closest to the Utopia Point is often selected as the 'best compromise design', whereas the extremes of the Pareto front are the 'best uncompromised designs'. Typically, these
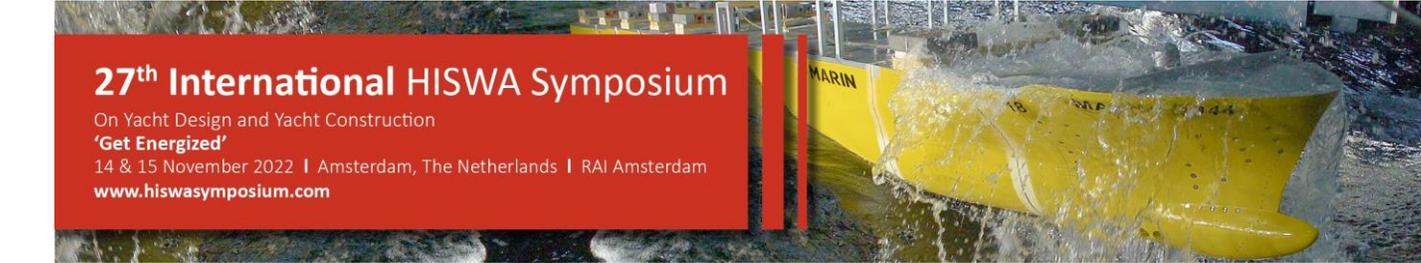
latter points are used to find the hull forms with the singular best resistance reductions at the speeds of interest. However, depending on the vessel's operational profile, as described in Section 2, the portion of time spent in each condition can influence the total energy demand over the course of the vessel's operating life, thus influencing the optimal hull selection. The effective power of the vessel, P_E, relates the vessel total resistance (R_T) and speed (V_s) by,

$$P_E = R_T \, V_s \tag{4}$$

Therefore, to quantify the operational contribution of each variant for each operating point (OP) in the use profiles, the parameter Lifetime Power Consumption (LPC), can be introduced as,

$$LPC = \sum_{i=1}^{OP} \left(P_{E,i} \cdot w_i \right) \quad \text{for } i = 1,2,\dots,OP \tag{5}$$

Where w_i is the proportion of time spent in each specific operation (see Section 2.1). Ultimately, the LPC function considers the total power demand during the entirety of the operational profile, which can then be relatively compared with that of the initial hull. Once the optimal hulls have been evaluated (step 13), selected points are to be chosen in order to undergo a re-evaluation which is necessary to verify the accuracy of the predictions obtained from the surrogates results. This leads to step 14 where the results from the surrogate and re-evaluated calm-water and added wave resistance are compared. If the differences between the two are acceptable in terms of the evaluated objective functions, the optimal design solution can be extracted for further detailed design (step 15). If the results are not acceptable, the evaluated points can be used to re-trained and enrich the dataset for further iterative optimisations.
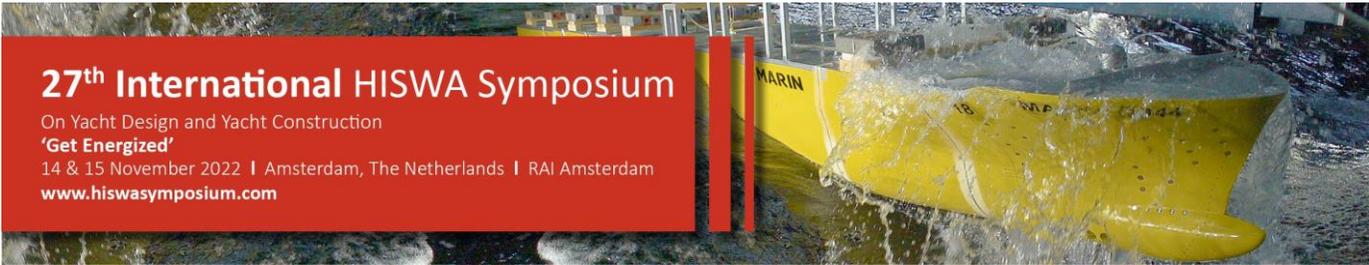
4. CASE INTRODUCTION

In this investigation, two existing Feadship yachts, subject A and B, are selected to undergo a re-optimisation process using the proposed methodology as described in Section 3. These selected hull forms were chosen as ideal candidates since they cover a broad size range and they both have been delivered recently. The corresponding hull shapes are presented in Figure 5, whereas, the main dimensions and selected hydrostatic parameters are given in Table 1.
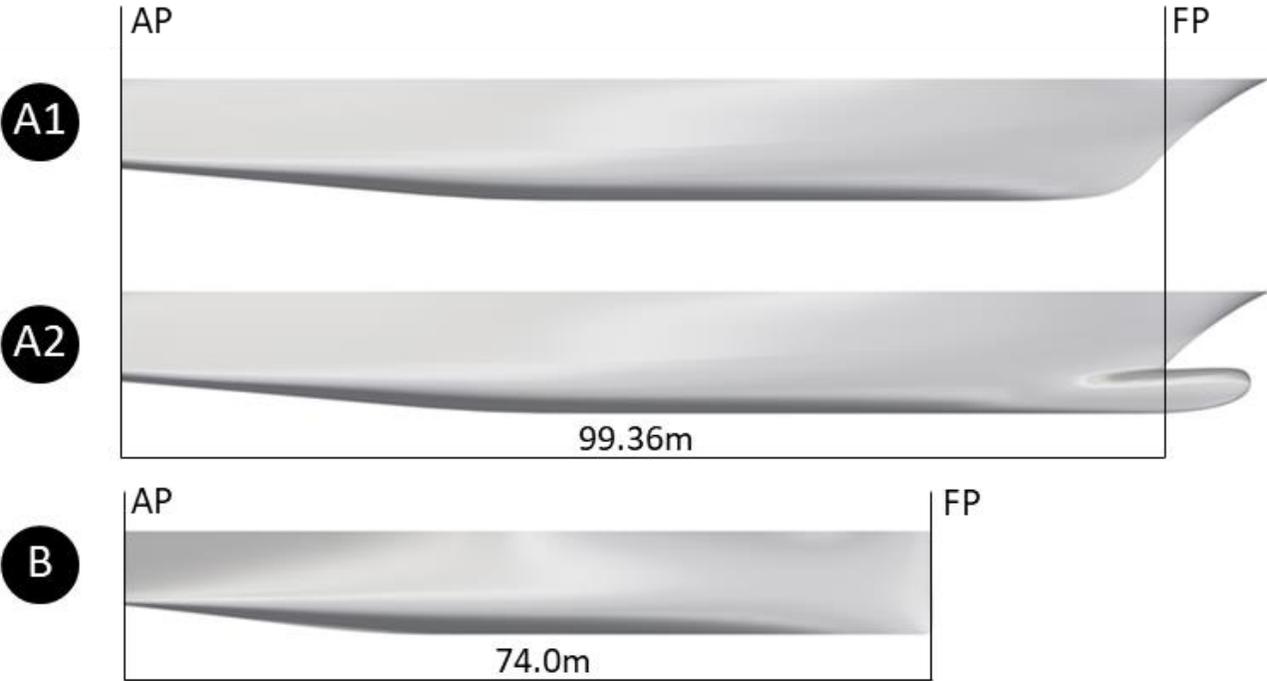
Figure 5: Parent hull geometries: (top) Yacht A1 original reference vessel; (middle) Yacht A2 reference vessel with bulb; (bottom) Yacht B original reference vessel. Aft perpendicular (AP) is set as St.0 and the fore perpendicular (FP) is set as St. 20 in both cases

These parent hulls were subject to an optimisation process during their original design conception, therefore they represent good starting points. This study focuses on two different phases within a typical Feadship design process. For Yacht A the early design (pre-contract) stage was considered, allowing more freedom in concept exploration. As such, the various ship characteristics such as bow shapes and main dimensions were varied more extensively and drastically to thoroughly explore the associated design space. Yacht B was considered within a more traditional basic design phase, where only localized and detailed changes could be applied. Typically such changes are dependent on physical design constraints or 'hard points'. More specifically for Yacht A, three bows were inspected; conventional, straight, and bulbous. However, two separate optimisations were conducted to ensure correct parameterization of the variations: one parent geometry focused on the straight and conventional bow features, whereas the other on the bulb parameters individually. The two geometries, as shown in Figure 5, are referred as Yacht A1 (No Bulb) and Yacht A2 (Bulb), respectively.

For each optimisation, the total resistance (in calm water and added wave conditions) at three different operating speeds were considered as objective functions for the surrogate based optimisation evaluations (see Section 2.1). In Table 1, the main parameters of the parent hulls are listed.
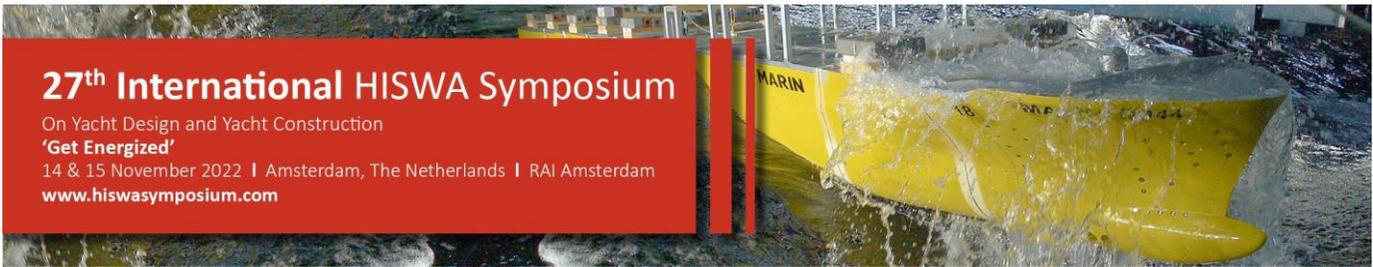
Table 1: Main dimensions and hydrostatic parameters of parent designs

Description	Symbol	Unit	Yacht A1 (Original)	Yacht A2 (Bulb)	Yacht B
Length between perpendiculars	L_{PP}	m	99.36	99.36	74.00
Breadth on waterline	B_{WL}	m	15.50	15.50	11.11
Mean draft	T	m	4.25	4.25	3.30
Displacement volume	$DISP_V$	m^3	3535.88	3670.91	1302.52
Block coefficient	C_B	-	0.54	0.56	0.48
Midship section coefficient	C_M	-	0.82	0.82	0.71
Prismatic coefficient	C_P	-	0.66	0.68	0.67
Fore Perpendicular to buoyancy center	FB	%L$_{PP}$	53.77	51.82	53.13
Transverse metacentre above baseline	KM	m	8.63	8.39	6.66

For the optimisation boundary conditions were defined to make sure the hull variant evaluated would comply design constraints such as stability, arrangement, weight and size/cost limitations. Bearing in mind the different design phases referred, the constraints were different for yacht A and B. In Table 2 the design constraints are listed.

Table 2: Design constraints

Description	Symbol	Unit	Yacht A	Yacht B
Length overall	L_{OA}	m	Not longer	Small increase due to integrated bulbous bow
Length waterline	L_{WL}	m	Variable	No variation
Volume	GT	m	Not smaller	Not smaller
Bow shape	-	-	3 options	Above water no change
Entrance angle		-	No constraint	No constraint
Bow radius	-	-	No constraint	No constraint
Bulbous bow width	-	-	Verify anchor arrangement	-
Water level above bulb	-	-	No constraint	-
Beam	-	-	No increase	No variation
Draught	-	-	No variation	No variation
Displacement	$DISP_V$	m^3	Not smaller	Not smaller
LCB	LCB	% L_{PP}	±0.5	±0.5
Metacentric height	KM	m	±0.1	±0.1
Water plane area	C_P	-	No constraint	No constraint
Front shoulder position	-	-	No constraint	No constraint
Aft shoulder position	-	-	Dominated by LCB constraint	Dominated by LCB constraint

4.1 Extreme variants and parameterizations

As described in Section 3.1, each hull undergoes a parameterization using a hull blending approach. Therefore, multiple extreme hull variants are required to be modelled. For each vessel optimisation, multiple changes associated to both the fore and aft body are included. A summary of each parameter can be seen listed in Table 3, for each associated design of experiments.

The selected parameters are decoupled from one another (to the best of our abilities), to ensure one variation change does not impact another. This helps to isolate and identify which design features play a prominent role within the optimisation. For instance, if the entrance angle reduction is dissociated from the stem extension, gains related to the extension feature variation as opposed to simply a reduction of the entrance angle is quantified instead. It should be noted, each parameterization is normalized between zero and one. Zero typically indicates the original reference/parent hull features, whereas the one indicates the extreme parameter change.
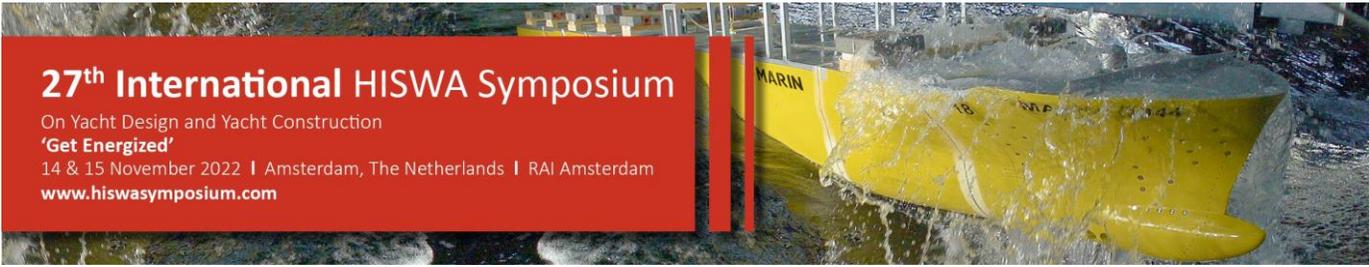
Table 3: Extreme design parameter descriptions and variations

Vessel Section	Design Parameter	Parameter Variation and Description
		DOE#1 – Yacht A1 original
Forebody	1. Stem extension	0 = straight bow (x = 109.6 from st.0) → 1 = initial bow (x = 99.3m from st.0)
	2. Entrance angle	0 = Initial angle (s = 0°) → 1 = min angle (s = -7.5°)
	3. Fore shoulder	0 = initial shoulder (s = 0m) → 1 = shift forward shoulder (s = +0.5m)
Aftbody	4. Buttock S-shape	0 = initial buttock (min s-shape) → 1 = maximum s-shape (integrated wedge)
	5. Bottom belly aft shift	0 = initial belly (x = 0m) → 1 = backwards belly shift (x = -2m)
	6. Stern waterline contraction	0 = initial stern (y = 0m) → 1 = stern contracts (y = -1.2m)
	7. V-transom (equal wet transom area)	0 = initial transom (z = 0m) → 1 = V-shape (z = -0.45m)
		DOE#2 – Yacht A2 with bulb (starting at St. 18)
Forebody	1. Bulb length	0 = max length (x = 107.8 from st.0) → 1 = min length (x = 103.0m from st.0)
	2. Bulb width	0 = max width (y = 1.62m from C.L) → 1 = min width (y = 1.20m from C.L)
	3. Bulb height	0 = max height (z = 4.30m from B.L) → 1 = min height (z = 3.50m from B.L)
	4. Bulb cross-section	0 = nabla (triangular) → 1 = cylindrical (circular)
	5. Entrance angle	0 = Initial angle (s = 0°) → 1 = min angle (s = -7.5°)
	6. Fore shoulder	0 = initial shoulder (x = 0m) → 1 = shift forward shoulder (x = +0.5m)
Aftbody	7. Buttock S-shape	0 = initial buttock (min s-shape) → 1 = maximum s-shape (integrated wedge)
	8. Bottom belly aft shift	0 = initial belly (x = 0m) → 1 = backwards belly shift (x = -2m)
	9. Stern waterline contraction	0 = initial stern (y = 0m) → 1 = stern contracts (y = -1.2m)
	10. V-transom (equal wet transom area)	0 = initial transom (z = 0m) → 1 = V-shape (z = -0.45m)
		DOE#3 – Yacht B original
Forebody	1. Entrance cusp	0 = Initial angle (x = 0m) → 1 = max cusp (x = -0.78m)
	2. Lackenby volume shift	0 = initial volume (x = 0m) → 1 = forward volume (x = +3.6m)
	3. Integrated bulb	0 = initial none (y = 0m from C.L) → 1 = max nabla bulb (y = 1.20m from C.L)
Aftbody	4. Stern tunnel	0 = initial tunnel (z = 0m) → 1 = no tunnel (z = -0.1m)
	5. Buttock S-shape	0 = initial buttock (min s-shape) → 1 = maximum s-shape (integrated wedge)
	6. Bottom belly aft shift	0 = initial belly (x = 0m) → 1 = backwards belly shift (x = -4.5m)
	7. Stern waterline contraction	0 = initial stern (y = 0m) → 1 = stern contracts (y = -0.3m)
	8. Transom bilge raise	0 = initial transom (z = 0m) → 1 = raised outer transom bilge (z = +0.12m)
	9. Transom midline lower	0 = initial transom (z = 0m) → 1 = lower transom midline (z = -0.27m)
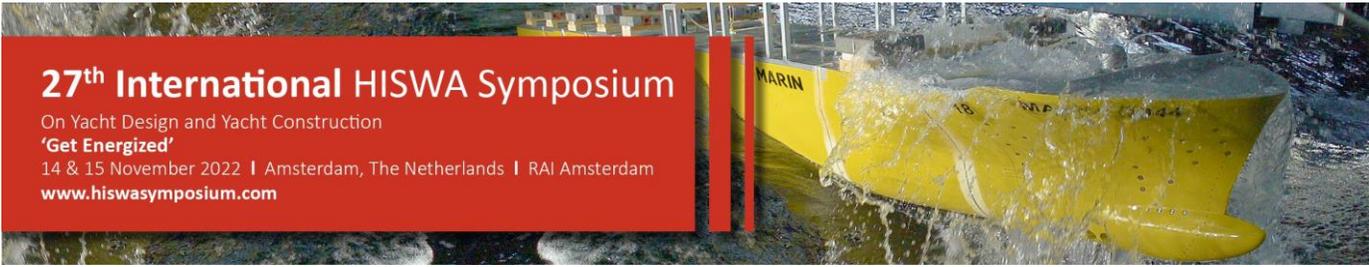
5. EVALUATIONS IN CALM WATER

The first evaluations focus purely on optimisation in calm water. Using the methodology described in Section 3 and parameterizations detailed in section 3.1, a full surrogate-based optimisation was performed. The corresponding 3D Pareto visualization results for both vessels can be seen in Figure 6. In addition to the conventional resistance metrics, total lifetime effective power consumption (LPC) is indicated for each hull variant. This metric applies the known operational distributions for each vessel (see section 2.1) to identify the regions on the Pareto front which perform best for that specific operation. While Yacht B considers a singular Pareto front, Yacht A is a combination of two separate optimisations to properly consider the impact of different bow configurations.
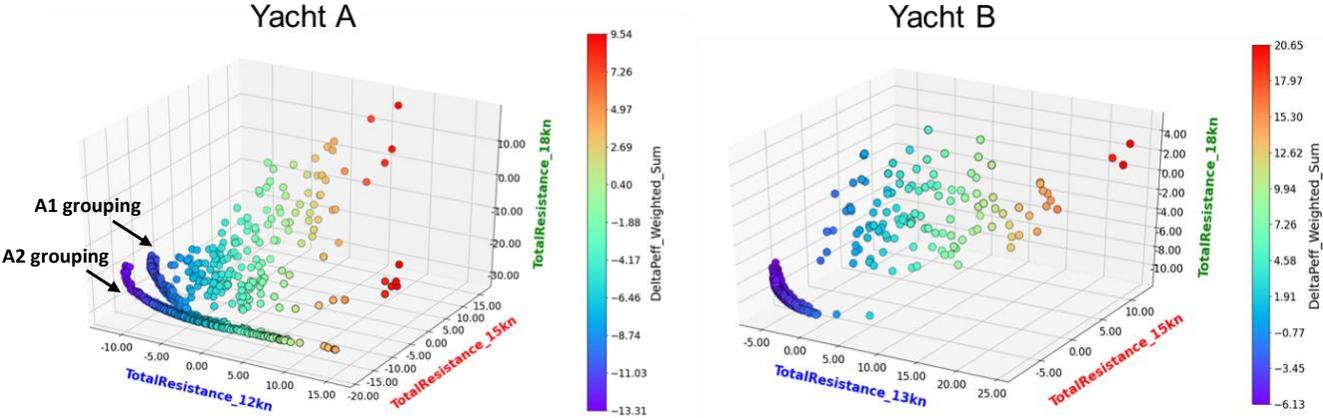
Figure 6: Surrogate based multi-objective genetic algorithm evaluated results in calm water conditions with lifetime effective power used as a comparative metric (see colored scale) for Yacht A (left) and Yacht B (right)

Focusing first on the Yacht A, the results indicate that a minimum power consumption corresponds to vessels demonstrating a near maximum resistance reduction at 12 knots. In this specific case, the bulb characteristics typically provide lower overall LPC for the given operating profile compared to the conventional and straight bow configurations (see the Pareto A2 grouping compared to the A1 grouping). When looking at Yacht B, we can see some similar trends in terms of operating speeds. Again, the results demonstrate a minimum LPC around the maximum resistance reduction favouring the lower speed regions. In both cases, the 15 knots outcomes do not have a large relative impact, as the spread in that dimension is marginal. Nevertheless, the trend indicates that hull variants with the lowest LPC do not advocate significant resistance reduction at top speeds. From the Pareto results, hull forms can thus be extracted and further investigated. In this study, two metrics are used to extract the 'optimal' variant:

- Minimum LPC (see Section 3.5)
- Minimum R_T at top speed (18 knots).

The first metric uses the given operational profile to quantify an operational impact, whereas the latter is what is traditionally used to optimise a vessel for contractual speed design. Using these objectives, a comparison between the extracted geometries is conducted. The values of the parameters (see Table 2) assumed for each relevant hull variant are summarized in Figure 7. Hull variants (A or B) followed by the indication "Peff (OP)" indicate the optimal cases for the minimum LPC, while hull variants followed by the indication "top speed" are related to the second metric.

For Yacht A, some interesting observations can be considered. Firstly, the bulb length, while relatively long for both analysis metrics, is slightly shorter for operation. However, the bulb width is much narrower. Furthermore, the cross-sections seem to deviate between more of a nabla shape when considering LPC and more cylindrical for top speeds in calm water. Other interesting observations are that the extreme limits of the s-shaped buttock are approached for the top speed. This feature in the extremes includes a semi-integrated wedge transom feature. Thus, such inclusion
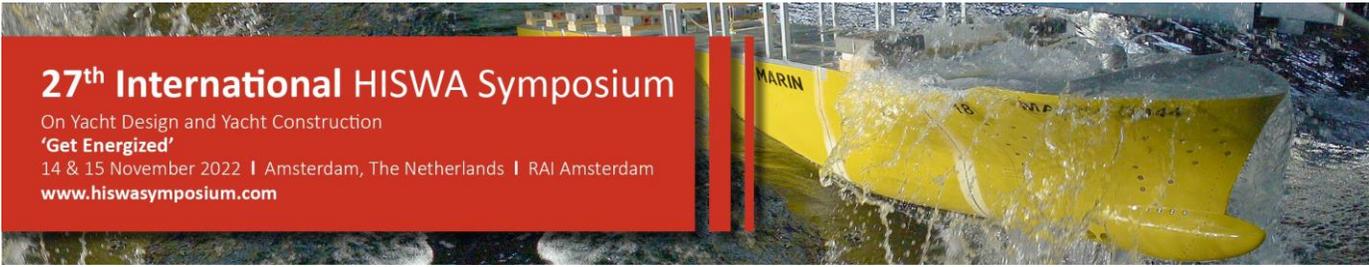
for top speeds is clearly favourable, supporting common hull design practices. However, results indicated that these wedge-like characteristics should not be considered when incorporating the operational profile.
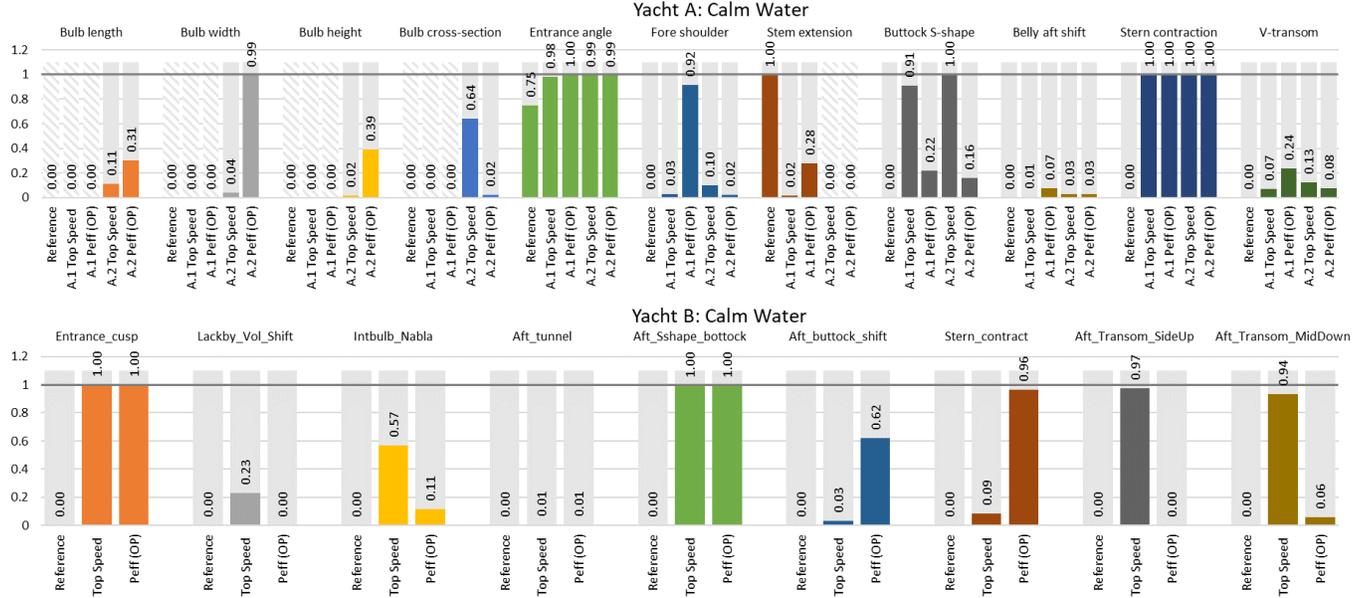
Figure 7: Hull parameter comparison for Yacht A (top) and Yacht B (bottom) in calm water conditions

When observing the stern, specifically the transom, the vessels prefer a maximum contraction in all cases. While an attempt was made to couple the stern contraction and V-transom to ensure a similar wetted transom area, some uncertainty exists about whether this objective was achieved. The reasoning was to decouple the effect of reducing viscous resistance with the reduction of the wetted transom area from the reduction of wave resistance linked to the pressure distribution at the transom. In the case of Yacht B, more localized modifications were considered. For both variants, a slight entrance cusp feature is favourable in calm water. Additionally, an integrated bulb seems more favourable for top speed designs than the current operational metrics. At the stern of Yacht B, while the extreme buttock S-shaped feature is shown for both variants, the geometry curvature is not as intense as the Yacht A case. Nevertheless, a slight wedge feature is still applied. However, when this feature is combined with the aft belly shift, the wedge is reduced, and a more flat transom is observed. Therefore, the role of the wedge is only applicable for the top speed variant, as demonstrated for Yacht A.
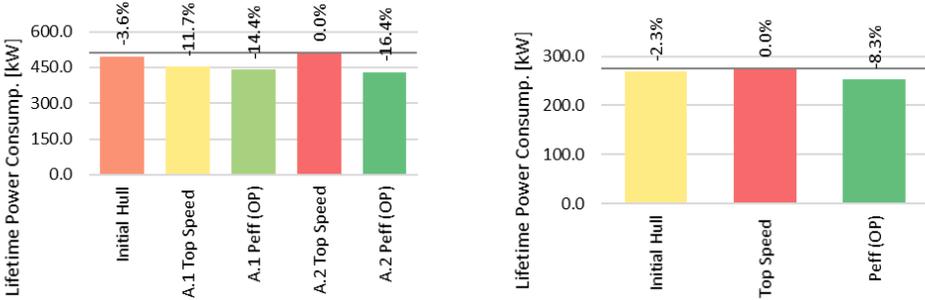
Figure 8: Lifetime effective power consumption comparison for Yacht A (left) and Yacht B (right) in calm water conditions

27th International HISWA Symposium
On Yacht Design and Yacht Construction
'Get Energized'
14 & 15 November 2022 I Amsterdam, The Netherlands I RAI Amsterdam
www.hiswasymposium.com

MARIN
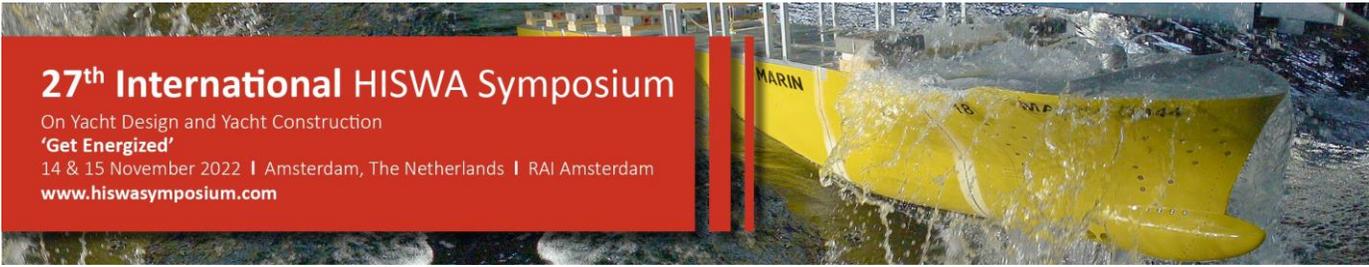
A complete comparison of the total LPC and relative speed impacts is visualized in Figure 8 and Figure 9, respectively. Here, a direct comparison between the various hull variants is considered. The hull variant optimal (lowest resistance) for the top speed was considered as a reference. Examining Yacht A, the inclusion of the bulb feature in the calm water condition gives the lowest LPC for the considered operational profile. In this case, a power reduction of approximately 12.8% is possible compared to the original vessel ("Initial Hull"). When considering the top speed, the bulb feature actually presents the worst LPC with a power use increase of approximately 3.6%. Yacht B shows similar trends, however, the overall impacts are much more marginal, which is merely due to more localized changes as opposed to the global changes considered in Yacht A. Nevertheless, a power reduction of approximately 6.0% can be obtained as compared to the initial hull.
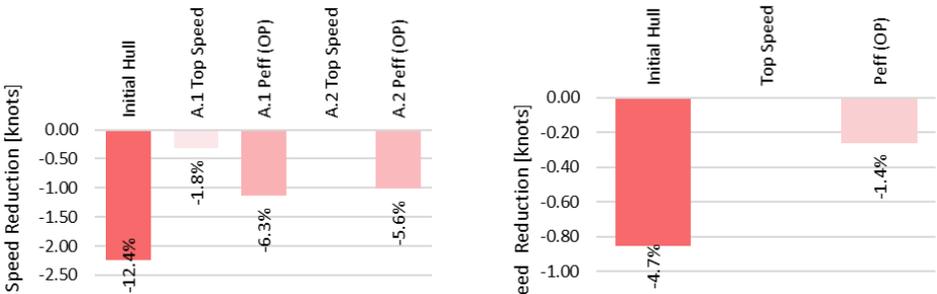
Figure 9: Optimal vessel comparison of the Impact on top speed for Yacht A (left) and Yacht B (right) in calm water conditions

Each vessel can also consider a relative impact on the top speed (18 knots). The resistance values along the speed range were approximated via direct curve-fitting interpolation. While there may be some uncertainty in the fitting of each point, the approach can provide a quick relative speed impact, which can be used in conjunction with LPC results to point out the trade-off between contractual and operational design aspects approximatively. In the case of Yacht A, it can be seen that the best performing LPC hull form indicates a speed reduction of approximately 1.0 knot as compared to the set reference vessel. Yacht B, on the other hand, indicates a marginal impact of 0.20 knots.

As noted in Section 4, general design constraints were considered for both cases. In the case of Yacht A, much more flexibility was given to explore the design space. Whereas in the case of Yacht B, the design is focused much more in the later stages, therefore, stricter constraints were considered. A summary of the various hydrostatic constraints for Yacht A and Yacht B and their reference values are presented in Table 4.

Table 4: Constraint comparisons where green values indicate that the constraints are met in calm water conditions

Constraints	Yacht A					Yacht B		
	Reference	A1 Top Speed	A1 Peff (OP)	A2 Top Speed	A2 Peff (OP)	Reference	Top Speed	Peff (OP)
KM [m]	8.63	8.39	8.44	8.31	8.38	6.66	6.70	6.58
$DISP_V$ [m3]	3535.88	3593.17	3700.93	3605.85	3570.06	1302.52	1296.09	1295.00
FB* [m]	53.42	51.13	51.36	50.78	52.41	39.75	38.65	39.59

*FB is defined as the longitudinal distance between the forward perpendicular and the centre of buoyancy

For Yacht A, only the displacement constraint is achieved. Both the KM and FB constraints are not adequately satisfied. In the case of the KM constraint, all new variants exhibit a smaller KM than the reference, with an average order of magnitude around 26cm lower. Whereas the FB deviations are an average of 2.0m forward. When Yacht B is considered, the only constraint fully achieved is the KM constraint. However, the differences between the other parameters are much narrower. In the case of the displacement constraint, there is only 7m³ from the minimum amount, whereas the FB shift is 0.10m from the acceptable constraint boundary. Ultimately, both vessels would require a second iteration of hull modifications, however, Yacht B would demand much less and easier modifications to achieve the established constraints.
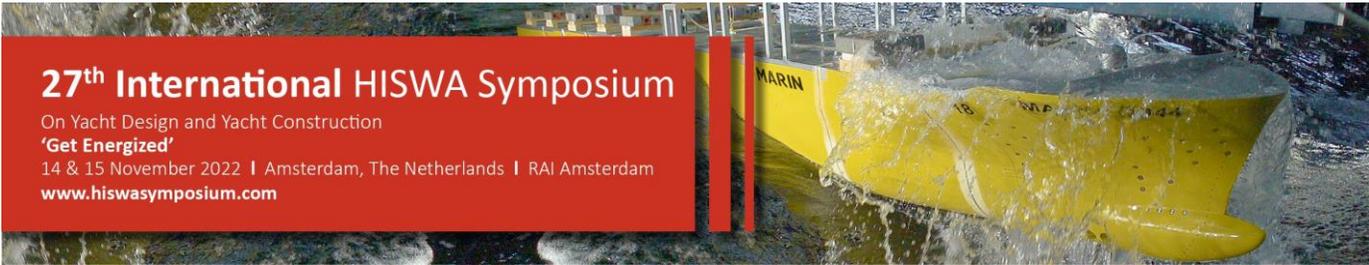
The following lines plans demonstrate the hull differences between the initial hull variant and the optimal vessels in calm water conditions (Yacht A and Yacht B are presented in Figure 10 and Figure 11, respectively).
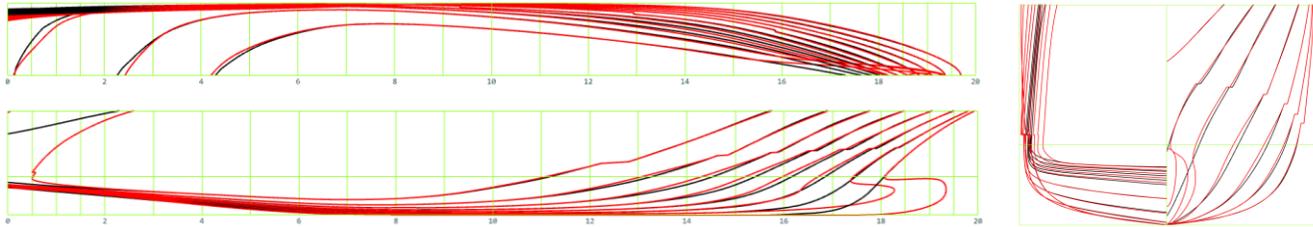
Figure 10: Optimal lines (red) compared with the reference vessel (black) for Yacht A in calm water conditions. Yacht A.2 Peff (OP).
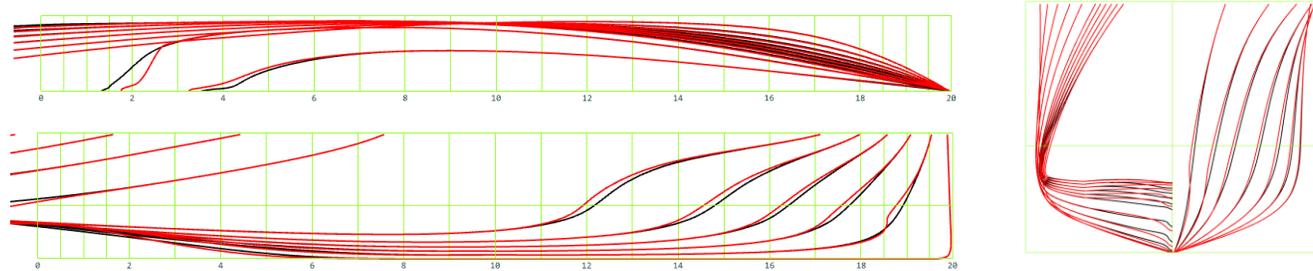
Figure 11: Optimal lines (red) compared with the reference vessel (black) for Yacht B in calm water conditions. Yacht B Peff (OP).

While these results are valid for the operating profile, alternative distributions of the operating profile itself can lead to entirely different outcomes and corresponding hull geometries. Therefore, great care and analysis should be conducted before applying such operational characteristics.
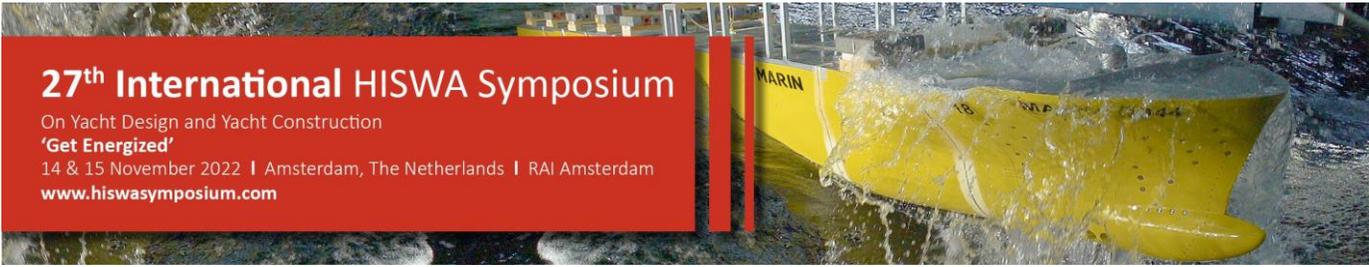
6. EVALUATIONS IN WAVE CONDITIONS

The second case focuses on the proposed research contributions to consider more realistic operating conditions in the optimisation process, therefore involving the impact of resistance in waves. Therefore, metrics, which consider the total resistance, consider the calm water and the added wave components. As a reminder, this section demonstrates the state-of-the-art while recognizing many factors of uncertainty exist (see Section 3.3). Thus, all corresponding results should be carefully considered and scrutinized to ensure that hydrodynamic sense is maintained.
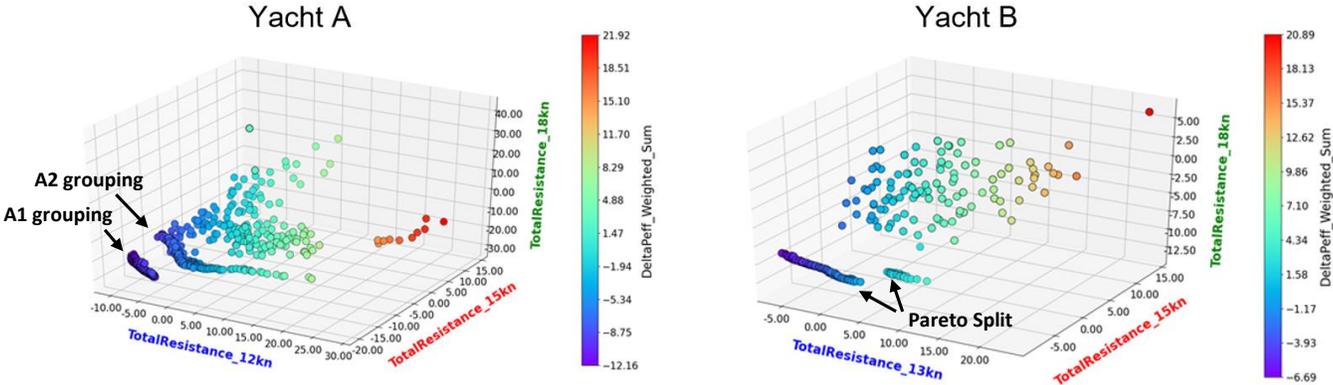
Figure 12: Surrogate based multi-objective genetic algorithm evaluated results in added wave conditions with lifetime effective power used as a comparative metric

As in the previous case, Yacht A and Yacht B are investigated. Using the methodology described within Section **Error! Reference source not found.**, the operational considerations in section 2.2, and parameterizations detailed in section 4, a complete surrogate-based optimisation was performed, where the corresponding 3D Pareto visualization results for both vessels in realistic conditions can be seen in Figure 12.

Once again, the evaluated Pareto fronts exhibit very similar characteristics to the calm water evaluations. However, some interesting differences are observed. When looking at the Yacht A case, the conventional straight bow characteristics (A1 Pareto indicated) now provide a lower overall LPC for the given operating profile compared to the bulbous bow configurations. When looking at Yacht B, we notice that there appears to be a slight split along the Pareto front. The cause of this irregularity is typically due to the optimisation developed response surface. Sometimes, solutions from the optimisation routine can be trapped in a separate local minimum region. This is the likely occurrence, however, due to the uncertainties in the SEACAL modelling approach (see Section 3.3), panelization errors could also be a contributing factor. While such uncertainty can influence results, investigation and research are ongoing to verify these results. Nevertheless, the findings of this section are still included in this paper to provide a global overview of the methodology and its potential. Using the same metrics described in Section 0, new optimal hull solutions can be extracted and compared, where the parameter results are shown in Figure 13.
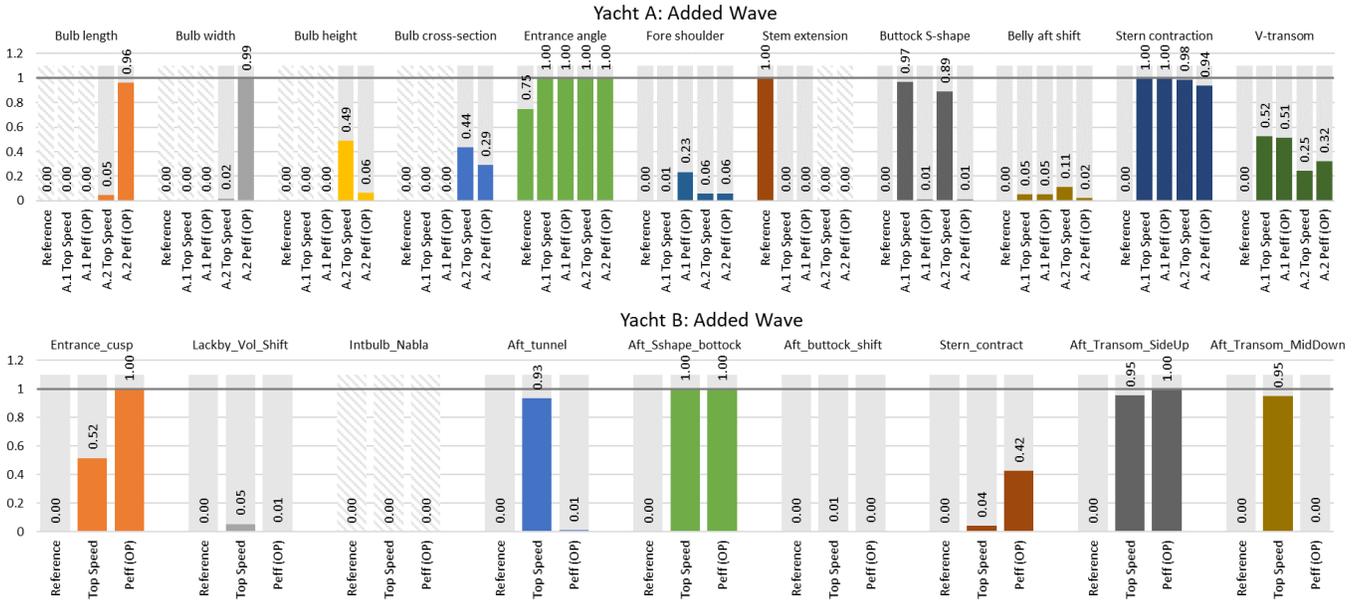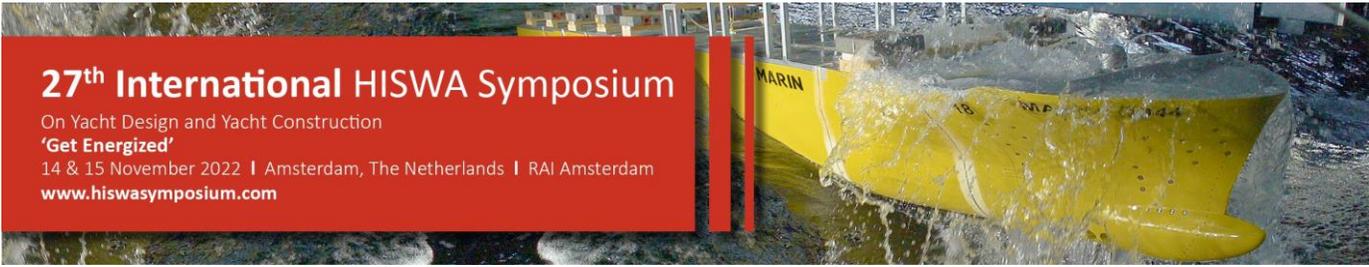
Figure 13: Hull parameter comparison for Yacht A (top) and Yacht B (bottom) in added wave conditions

Based on the results for Yacht A, some interesting differences can be considered in comparison with the calm water analysis. Firstly, the bulb lengths, which were quite long within the calm water analysis, now show that a minimum bulb length is favoured for minimum LPC. This minimum bulb length links to the stem extension, where a completely straight bow is preferred in added wave conditions. Again in the calm water condition, the transom features greatly favour the stern contraction. However, a slightly more V-shape is preferred across all extracted optimal geometries in this case. Ultimately, it can be observed that much similarity is observed between the top speed vessel shapes in both calm water and waves. Nevertheless, the major differences are related to the bulb height and cross-section, which appears to decrease in height and transition to a more nabla shape. Based on practical engineering experience, a more cylindrical cross-section is expected to be a favoured solution. This expectation is based on current market trends, where bulb designs approach more torpedo-like profiles when considering a broad range of operations and speeds. Thus, further investigation should be considered to validate if the corresponding added wave trends are accurate in this case.

In the case of Yacht B, more interesting differences are observed. In this specific study, in an attempt to avoid panelization discrepancies, the integrated bulb feature was not considered. Thus, eliminating a significant source of modelling uncertainty. Based on the results, the main differences between calm water and added wave conditions are related to the transom parameters. While the two vessels (optimised respectively, one for the top speed and the other for the operating profile) generally exhibit similar trends to the calm water scenario, discrepancies in the tunnel, buttock shift, stern contraction and transom bilge raises are noticed. These changes ultimately produce a non-conventional transom shape where a semi-singular tunnel feature is produced. Such transom shapes are not conventional and slightly counterintuitive regarding hydrodynamic principles when considering twin-shaft arrangments. Thus, further research is necessary to validate such irregular transom shapes.

27th International HISWA Symposium

On Yacht Design and Yacht Construction
'Get Energized'
14 & 15 November 2022 | Amsterdam, The Netherlands | RAI Amsterdam
www.hiswasymposium.com
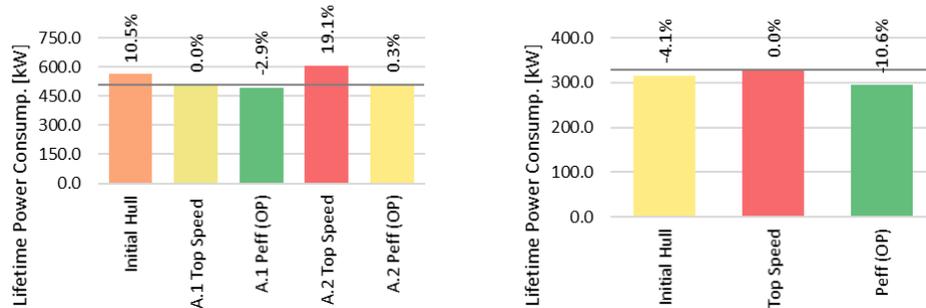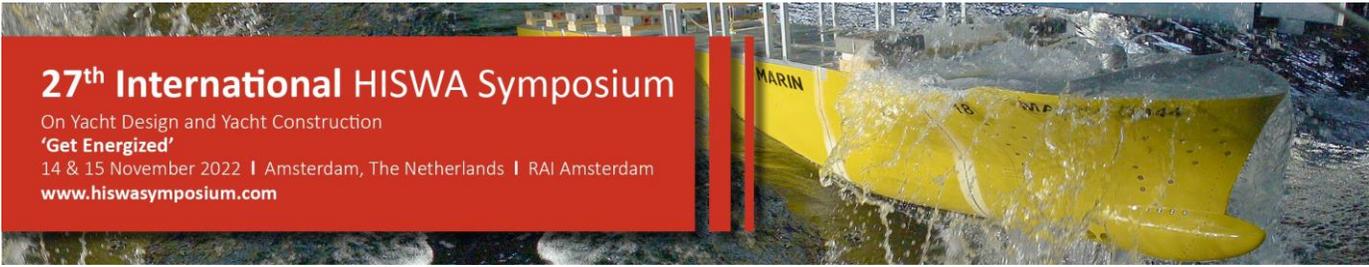
Figure 14: Lifetime effective power consumption comparison for Yacht A (left) and Yacht B (right) in added wave conditions

A comparison of total LPC and relative speed impacts is visualized in Figure 14 and Figure 15, respectively. In the added wave condition, the straight bow feature (A.1 Peff (OP)) presents the lowest LPC for the considered operational profile. In this case, a power reduction of approximately 13.4% compared to the initial hull is achieved. This is approximately 1% less than its calm water counterpart. When considering the best hull for top speed, the bulb feature, once again, presents the worst LPC with a lifetime power increase of approximately 9% and 22% as compared to the initial hull and best LPC vessel, respectively. Yacht B presents similar trends with a power reduction of approximately 6.5% compared to the initial vessel, which is about 0.5% more than in the calm water condition.
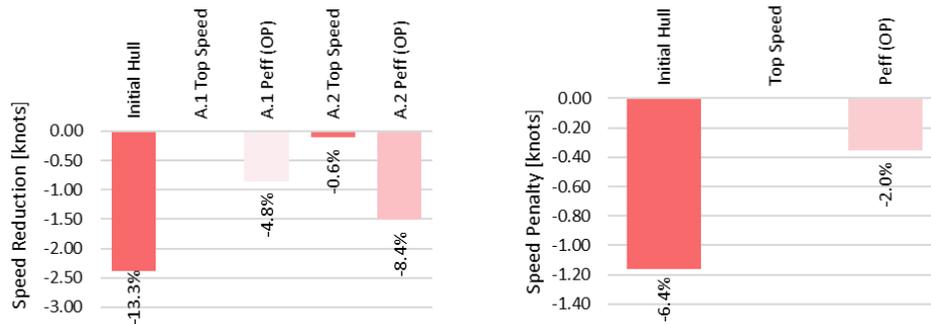
Figure 15: Optimal vessel comparison of the Impact on top speed for Yacht A (left) and Yacht B (right) in added wave conditions

The impacts on top speed are identified using a similar approach as demonstrated in the calm water cases. In the case of Yacht A, the best performing LPC hull form indicates a speed reduction of approximately 0.7 knots as compared to the set reference vessel. Yacht B, on the other hand, suggests an impact of 0.38 knots. In both cases, the impacts on speed are relatively similar as compared to the calm water investigation. As previously detailed, a series of vessel constraints were to be followed. A summary of the various hydrostatic constraints for Yacht A and Yacht B in relation to their references is seen in Table 4.

Table 5: Constraint comparisons where green values indicate that the constraints are met for added wave conditions

Constraint	Yacht A					Yacht B		
	Reference	A1 Top Speed	A1 Peff (OP)	A2 Top Speed	A2 Peff (OP)	Reference	Top Speed	Peff (OP)
KM [m]	8.63	8.39	8.35	8.30	8.42	6.66	6.70	6.68
$DISP_V$ [m3]	3535.88	3588.44	3658.06	3605.07	3558.57	1302.52	1287.02	1275.81
FB [m]	53.42	51.11	51.64	51.05	52.79	39.75	39.51	39.40

*FB is defined as the longitudinal distance between the forward perpendicular and the centre of buoyancy

Again, for Yacht A, only the displacement constraint is achieved. Compared with the calm water case, the other metrics, KM and FB, are not satisfied within similar orders of magnitude. However, the KM and FB constraints are
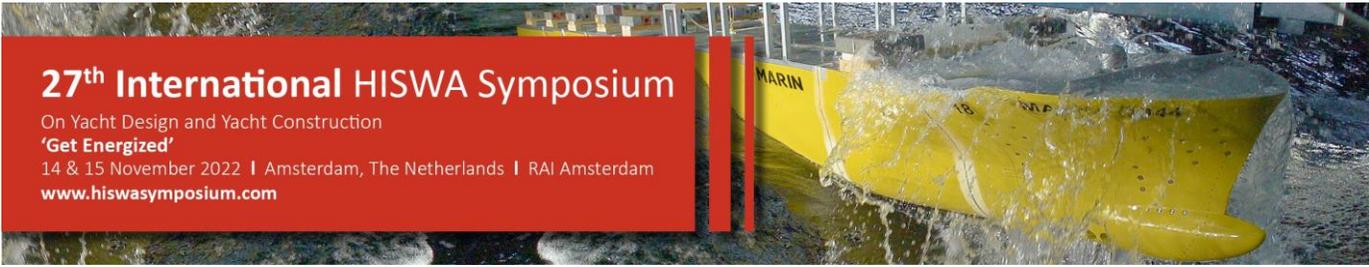
achieved when Yacht B is considered. In comparison, the displacement constraint, in this case, is much lighter, where an average of 20m^3 from the acceptable constraint boundary is shown. While the constraints for Yacht B are nearly achieved, both vessels would require a second iteration of hull modifications.

The corresponding lines plan, which demonstrates the hull differences between the optimal vessels in added wave conditions for Yacht A and Yacht B, can be seen in Figure 16 and Figure 17, respectively.
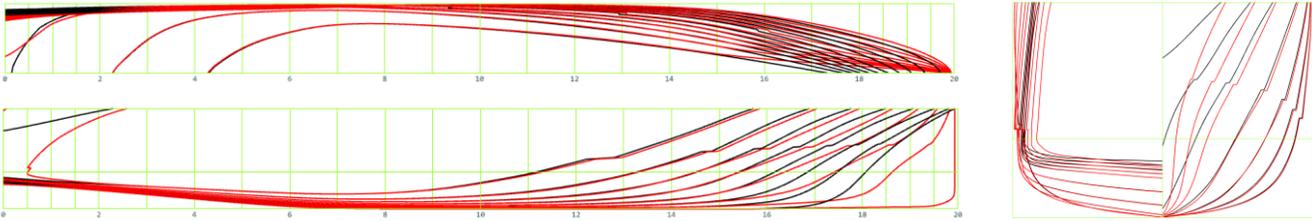
Figure 16: Optimal lines (red) compared with the reference vessel (black) for Yacht A in added waves. Yacht A.1 Peff (OP).
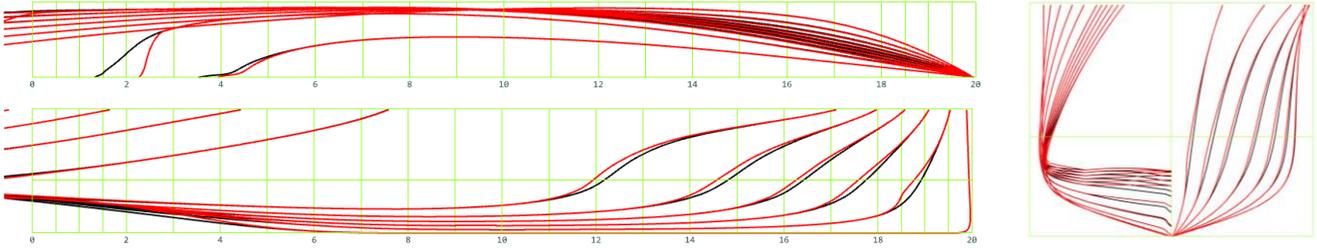
Figure 17: Optimal lines (red) compared with the reference vessel (black) for Yacht B in added wave conditions. Yacht B Peff (OP).
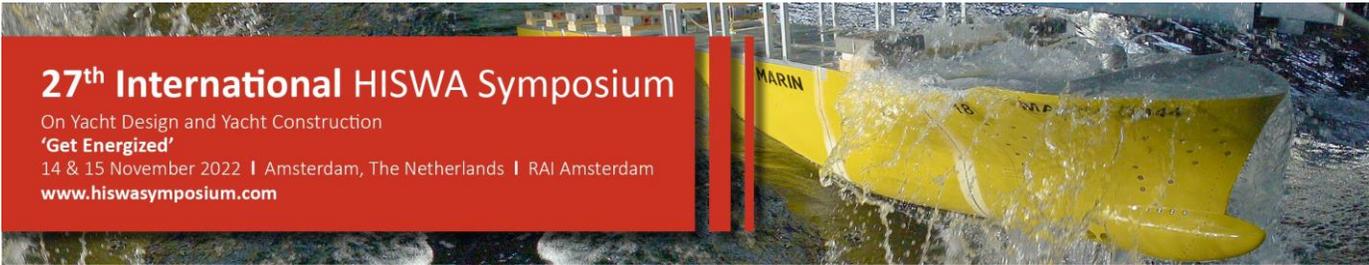
7. DISCUSSION, CONCLUSIONS AND RECOMMENDATIONS

The optimisation process has shown that some substantial lifetime power reductions can be achieved w.r.t. the as-built hulls. Where the yachts A and B optimized shape reductions were -12.8% (A.2), -6.0% (B) and -13.4% (A.1), -6.5% (B) for calm water and added waves, respectively. These reductions come with impacts on aesthetical considerations with respect to the, for instance, bow shapes (Yacht A) and minor waterline tapering (Yacht B). Negative impacts in relation to vessel top speed are also observed, where reductions 1.0 knot (A.2), 0.2 knots (B) and 0.70 knots (A.1), and 0.38 knots (B) for calm water and added waves, respectively. However, these optimisation impacts are without considering either the CAPEX or OPEX benefits.

The impact and cost reductions can be estimated based on an annual use profile and energy consumption. A case example for Yacht A is calculated based on actual energy consumption feedback, known specific emissions, and fuel cost, which are then compared to alternative efficiency improvements estimated based on previous work [12] and recent engineering results. The lifetime a yacht is conservatively expected to be 30 years. Table 6 provides the environmental impact and cost-saving estimation assuming fossil diesel (EN590) at a fuel rate of 1000 euro per m^3. The global warming potential (GWP) is estimated based on a specific well-to-wake emission of 3.9 t CO_2-e/t EN590 fuel [13].

Table 6: Lifetime (30 years) operational GWP reduction and cost-saving estimation (Yacht A):

Efficiency improvement	Global Warming Potential (GWP)	CAPEX + OPEX
	kt CO_2-e	k€
Operation based optimisation	7.85 (-7%)	-2397
Waste Heat Recovery	5.77 (-5%)	-1263
Improved insulation	2.89 (-3%)	-831
Electrical stabilizer	2.31 (-2%)	-505
Solar PV 250m^2	2.89 (-3%)	-481

When non-fossil diesel or other alternative fuels are used, the reduction in GWP will be considerably lowered towards net zero. However, the operating cost reduction may be much more significant depending on fuel cost and emission taxation developments. A double fuel rate is often used as a best first estimate.

Based on the study presented, the following general conclusions can be drawn:
- The methodology presents a flexible and computationally efficient way to incorporate operational information within the design optimisation phases, where constraints may be varied depending on the design phase.
- GWP and OPEX cost reductions are very significant without any additional CAPEX.
- Added resistance estimations are challenging to assess with confidence – can lead to misleading trends and general conclusions. The scope of the analysis domain is widening; therefore, simplifications are very significant.

Recommendations for further developments and yacht design implementation are:
- Only a single added resistance component is considered – added waves. Additional added resistance components such as wind and bio-fouling variance should be additionally explored.
- Only a single operational condition is considered. In the future, the full radial (360-degree) spectrum wave should be considered in conjunction with a whole route operational profile.
- Constraints should be integrated into the optimisation algorithm. Thus, solutions such as displacement compensation and/or constraint-surrogate intersection modelling should be considered.
- Extend philosophy to the hotel load optimisation of a superyacht.

Finally, an additional recommendation should be implemented for altering a yacht's new-build specification based on the current findings. Currently, sea trial requirements serve a contractual purpose between the yard and client. However, this study proves that this leads to subpar performance within the actual operation. Alternatively, the speed profile and fuel consumption can be specified using the proposed methodology as a basis, then verified at the most
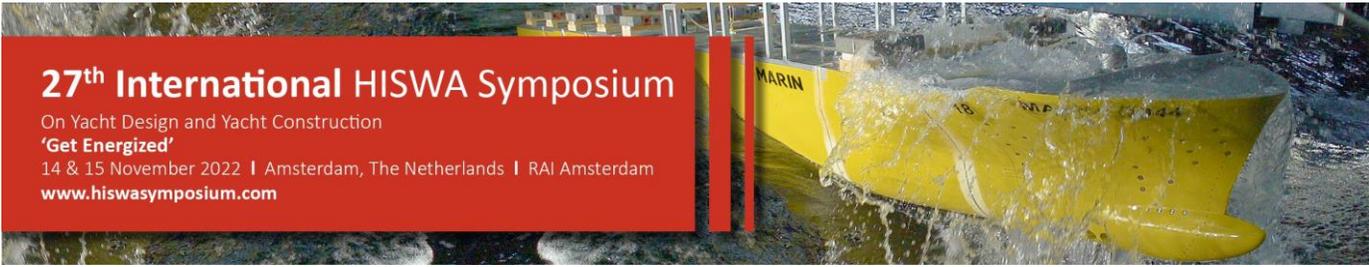
critical speeds during the sea trial and corrected for calm water conditions. Analogous to the contractual condition, the study introduces a relevant case regarding energy efficiency design index certification (EEDI). Current MARPOL regulations are applied to REG-YC Part B vessels, which consider a fixed speed at 75% installed MCR. Instead, an operational-based approach could be adopted to distinguish actual efficiency-enhancing measures, thus collectively reducing propulsion and hotel energy use and related environmental impacts.

REFERENCES

[1]   Adams, B. M., Ebeida, M. S., Eldred, M. S., Geraci, G., Jakeman, J. D., Maupin, K. A., Wildey, T. (2018). Dakota, a multi-level parallel object-oriented framework for design optimisation, parameter estimation, uncertainty quantification, and sensitivity analysis: Version 6.9 User's manual. Sandia Technical Report SAND2014-4633.

[2]   Bougis, J. (1981). Asymptotic study of the wave filed generated by a steadily moving pulsating source. Laboratoire d'Hydrodynmaique Navale.

[3]   H. Zakerdoost, H. (2018). Application of variable-fidelity hydrodynamic optimisation strategy in fuel-efficient ship design. Journal of Mechanical Engineering Science (IMechE)(Hydrodynamics of Marine Propulsion).

[4]   MAN Diesel & Turbo. (2012). Basic principles of ship propulsion. MAN Energy Solutions. Copenhagen, Denmark.

[5]   Maritime Research Institute Netherlands (MARIN). (2020). ReFRESCO Web page. Retrieved from https://www.refresco.org.

[6]   Maritime Research Institute Netherlands (MARIN). (2021). SEACAL version 5.0.0: Theory manual. MARIN RD report.

[7]   Raven, H. (2018). Minimising ship after body wave making using multi-fidelity techniques. 32nd Symposium on Naval Hydrodynamics.

[8]   Raven, H., & Scholcz, T. (2017). Wave resistance minimisation in practical ship design. VII international conference on computational methods in marine engineering.

[9]   Rhino version 6 SR10. (n.d.). Retrieved from https://www.rhino3d.com/download/Rhino/6.0/release.

[10]   Scholcz, T., & Dalen, E. F. (2020). Surrogate-based multi-objective optimisation for powering and seakeeping. Practical design of ships and other floating structures (PRADS).

[11]   Vaz, G., Jaouen, F., & Hoekstra, M. (2009). Free-surface viscous flow computations. Validation of URANS code FRESCO. Proceedings of OMAE2009.

[12]   Van Vliet, N. (2021). Green Refits: Reducing yacht operational emissions through refitting. TU-Delft master thesis.

[13]   Harmsen J., Nesterova N., Bekdemir C., Kranenburg K. van. (2020) TNO report TNO 2019 R11732 Green Maritime Methanol WP2 Initiation and Benchmark analysis.